Prediction of Cavitation Erosion by Detached Eddy Simulation (DES) and its Validation against Model and Ship Scale Results

Dr. Dmitriy Ponkratov[1], Alejandro Caldas[2]

[1, 2] Technical Investigation Department (TID), Lloyd's Register, London, UK

ABSTRACT

Currently Computational Fluid Dynamics (CFD) demonstrates comparatively good results in prediction of cavitation, however, from a practical point of view it is important to understand whether the simulated cavitation is erosive or not. This can provide propeller and ship designers with an additional confidence at an initial stage of the design process. The existing estimations of cavitation erosion are usually based on the model tests performed in a cavitation tunnel by the implementation of a soft paint on the propeller surface. Although this method has been validated for conventional propellers, Lloyd's Register Technical Investigation Department (LR TID) witnessed some cases when it did not work satisfactorily for propellers with moderate to high geometrical characteristics and propellers with energy saving devices. Undoubtedly, one of the reasons is a difference in Reynolds numbers in model and full scale cases. The main objective of the current study is to develop a method for numerical erosion prediction which is effective across a range of Reynolds numbers (model scale and full scale).

KEYWORDS

CFD, DES, Cavitation, Erosion.

1. INTRODUCTION

It is well known that cavitation erosion is a difficult physical phenomenon that needs a considerable amount of effort to fully understand and accurately predict. In its quest to raise safety and quality of new ship designs, whilst improving performance efficiency and reducing environmental impact, both for marine environment and people on board, researchers are deeply involved with continued research in issues related to cavitation and erosion.

In addition to the propeller efficiency, the main concern of ship-owners and operators is erosion induced by cavitation. Hence, an accurate numerical prediction of erosion at the design stage is a very powerful tool and many researchers put their efforts into investigating this phenomenon and developing an algorithm for its prediction. Two main methods for cavitation and erosion investigations using CFD should be highlighted.

One method represents an attempt to fully resolve the cavitation phenomenon numerically. This approach is being developed by Schmidt et al. (2007), Schmidt et al. (2008), Schmidt et al. (2009), Mihatsch et al. (2013). It should be noted that the compressibility of the fluid is taken into consideration in their simulations, however the liquid is inviscid. In general, this approach requires a very fine computational mesh in order to capture all scales of cavitation events. When the main focus is related to erosion prediction, a physical simulation of shock waves near an object surface is required. As the speed of propagation of this event in the water is very high, an extremely accurate mesh (the size of every cell less than 1 mm), together with a minute time step (approximately 10^{-7} -10^{-8} sec), has to be applied. As a result, the calculation time of a model scale object can take up to 1 month using 192 processors (Schmidt et al. (2009)). Undoubtedly, the cavitation resolution is very accurate from the physical point of view as it takes into account the simulation of all types of erosion events. Moreover, as shown in (Schmidt et al. (2009)) the pressure foot prints of shock waves predict the location of potential erosion relatively accurately. However, the practical implementation is very limited, as a simulation of full scale realistic objects, such as a marine propeller, would take too much time.

The second approach is related to the implementation of erosive functions or erosive indices. The main idea of this method is not to resolve all cavitation behaviours numerically but to predict possible impacts by numerical functions. For example, Nohmi et al. (2008), Hasuike et al. (2009) developed four indices which are based on pressure and volume fraction time derivatives as well as

absolute pressure difference. Further investigation of this approach was completed by Li Ziru in his PhD thesis (Li (2012a) and Li et al. (2012b)), where the aforementioned indices were studied and another index was introduced. Lloyd's Register Technical Investigation Department (LR TID) has developed its own erosive functions which were reported in (Boorsma et al. (2011)). The principal difference of this approach is that there are no critical requirements to cell size and time step, other than to resolve the macroscopic cavitating flow phenomena, in order that the calculation time becomes more reasonable. The standard setup for this approach is incompressible flow with viscous effects. However, it should be highlighted that this approach may not fully represent the physical details of cavitation flow; therefore the predictions may not be sufficiently accurate. Some attempts at further development of this approach were made within the current study. As a result, the more sophisticated DES model has been used for model and ship scale cases, and also some new erosive functions have been developed.

2. EROSION MODELLLING FUNCTIONS

As part of this study, various theories on how best to determine erosive potential from the parameters available in the current flow field and cavitation models have been examined. These methods do not consider the material-related aspects of the cavitation-erosion process, which are also critical, but aim to provide a qualitative, or relative quantitative, estimate of the erosive potential of the flow. As mentioned earlier, some functions studied in this project were the functions developed in LR TID and reported in (Boorsma et al. (2011)). In addition, some new erosive functions have also been developed during the study. The total number of functions was twelve; however, not all of them presented good results. The results of the most promising functions (№1, 5 and 8) are presented in this paper. The publication of these functions in this paper is withheld pending further validation work. Each function was created in two forms taking into account the physics of cavitation phenomena. It is well known that erosion damage can be caused either by significant instantaneous cavity collapse or by a series of collapses with moderate amplitude. The second mechanism is somewhat similar to fatigue phenomena. In order to investigate both mechanisms, two different quantities based on all erosive functions have been created. The first quantity reflects the maximum value of the function at every surface cell of the object within one shedding cycle; hence it takes into account a power of instantaneous impact. The second quantity shows the accumulated value of the function within one shedding, cycle; hence it shows the integrated values over the cycle. The functions were validated with several study cases. All CFD simulations reported in this work were performed using STAR-CCM+, a general purpose, commercial CFD code, based on the finite volume method. The two-phase flow was modelled using the volume-of-fluid (VOF) method with cavitation growth and collapse represented using the simplified Rayleigh-Plesset equation.

3. STUDY CASES

3.1. MODEL SCALE: HYDROFOIL NACA0015

As a CFD simulation of cavitation requires fine mesh, together with a small time step, it was decided to validate the existing erosion functions and develop new ones based on a model scale object. This allowed the investigation of the numerical functions within a reasonable time frame. For the initial study case an intensively investigated hydrofoil NACA0015 was selected. Numerical and experimental studies for this case were completed within Cooperative Research Ships (CRS) EROSION II working group in which LR TID participated (Boorsma (2010), Hoekstra (2011) and Rijsbergen et al. (2011)).

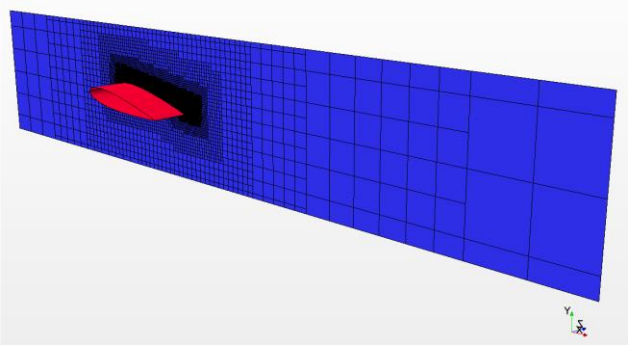

Figure 1. Computational domain identical to cavitation tunnel working section.

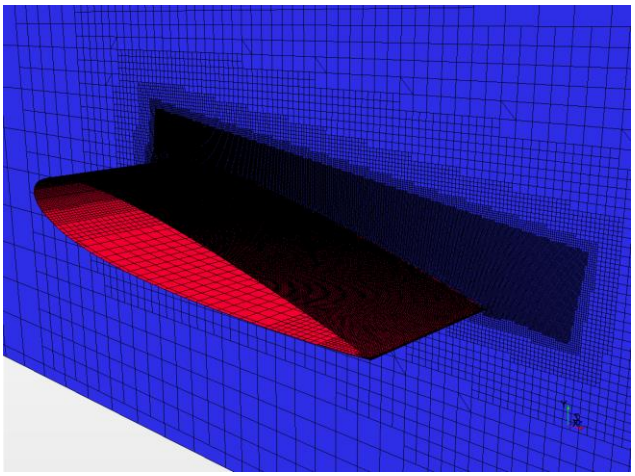

Figure 2. Mesh refinement above the foil.

As the hydrofoil has a well-known offset of points, the geometry was built based on these points. The size of computational domain was identical to section of the cavitation tunnel where the object was tested. An illustration of the computational domain is provided in **Figure 1**.

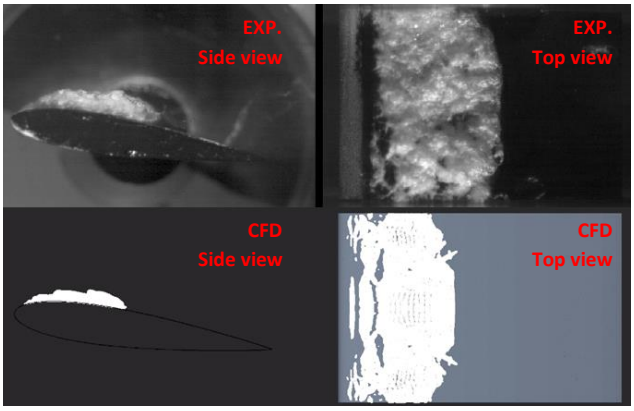

Figure 3. Cavitation predicted by CFD vs Experimental observation. Solution time 0.084415 s.

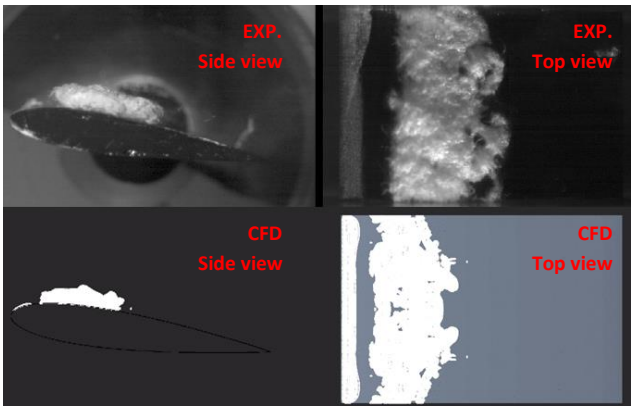

Figure 4. Cavitation predicted by CFD vs Experimental observation. Solution time 0.084825 s.

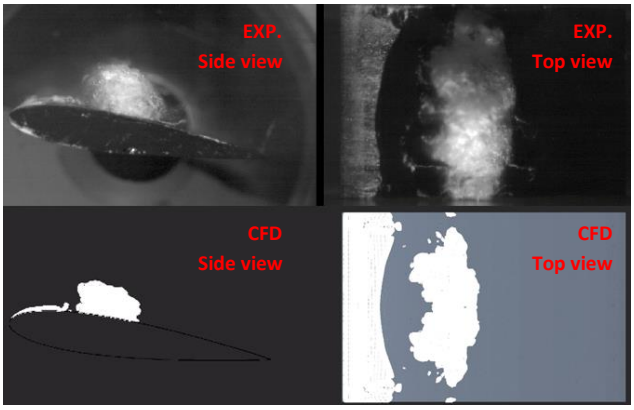

Figure 5. Cavitation predicted by CFD vs Experimental observation. Solution time 0.085595 s.

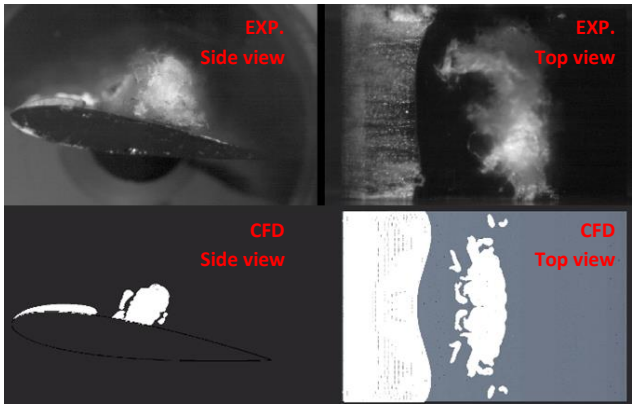

Figure 6. Cavitation predicted by CFD vs Experimental observation. Solution time 0.086245 s.

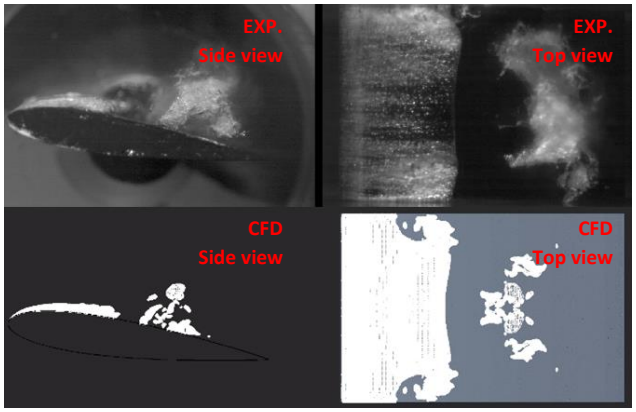

Figure 7. Cavitation predicted by CFD vs Experimental observation. Solution time 0.087245 s.

The computational domain extended to approximately two foil lengths fore of the leading edge, four lengths aft of the trailing edge and on the sides the foil was connected to the walls. As the cavitation simulations require a very fine mesh and the main focus of the work was erosion prediction, it was decided to calculate only half a foil, assuming that cavitation extent is symmetrical. A trimmed mesh was used and an additional mesh refinement was made on the upper side of the foil where the cavitation structures were expected (**Figure 2**). The final computational mesh was about 4 million cells. Initial calculations were completed with RANS equations and closed with the k-ω SST turbulence model. However, the final calculations were completed with Detached Eddy Simulation (DES) model. The computational settings, such as flow speed, cavitation number, and angle of attack were identical to the experiment set up.

The simulation strategy was as follows: at the initial stage the flow around the hydrofoil was calculated in a steady mode. The cavitation model was active; however, the saturation pressure was set to an unphysical value to ensure that cavitation does not appear at this stage. Once the

convergence of this stage is achieved, the simulation was switched to an unsteady mode maintaining the same unphysical saturation pressure. The time step at this stage was approximately $2.0x10^{-5}$ sec and the simulation was continued. As soon as the unsteady case converged, the time step was reduced to $1x10^{-6}$ sec and saturation pressure was set up to a physical value. As sudden development of cavitation may be unphysical, no erosion functions were activated at this stage. After some shedding cycles are completed, it was assumed that cavitation is stabilised and the erosion functions were activated. **Figures 3** to **7** show the development of cavitation during one shedding cycle. It can be noted that the cavitation extent is underestimated by CFD: even though the shape of cavitation cloud is similar to that observed in the experiment, the volume of this cloud is under predicted. Moreover, the collapse of the cavitation cloud occurs near the mid chord area in CFD, but in the experiment it occurs closer to the trailing edge of the foil. As a result, five main zones of paint damage were identified after the test in the cavitation tunnel. The first four zones are related to areas where the substructures separated from the main sheet cavity collapsed (**Figure 8**). The last one, closer to the trailing edge, is the zone where the primary cloud directly shed from the main sheet cavity collapsed.

It should be highlighted that the paint removal presented in **Figure 8** was observed after 30 min test in the cavitation tunnel. Undoubtedly, a CFD simulation of the full duration of the test would not be practical, as it could take too long to compute. In the current study it is assumed that damage over the one shedding cycle is similar to others, hence, the erosion functions were activated only for the duration of one shedding cycle.

All twelve erosion functions were activated for this case; however, **Figures 9** to **11** show only results of Functions 1, 5 and 8 which demonstrated the best predictions. It can be seen that all zones are identified reasonably well; however, their locations are slightly further from the trailing edge than observed in the test. This is due to the fact that cavitation structures collapsed earlier in the CFD prediction than in the model test. Despite the fact that the cavitation behaviour on the foil is somewhat underestimated by CFD, the erosion functions displayed good performance as they accurately identified the locations of cavities collapse. Further improvement of cavitation behaviour on the foil may result in erosion zones coming even closer to model scale predictions. As the main goal of the current study was to investigate the erosion effect of cavitation, it was concluded that the developed functions were able to correctly identify the zones of paint removal on a model scale object.

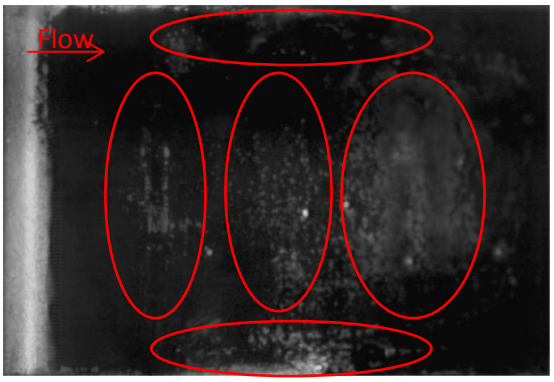

Figure 8. Paint removal after the model tests.

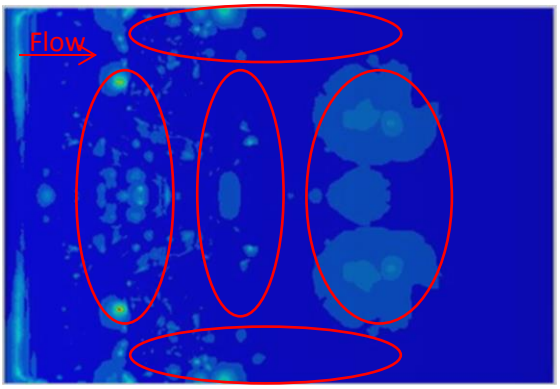

Figure 9. Erosion zones predicted by Function 1.

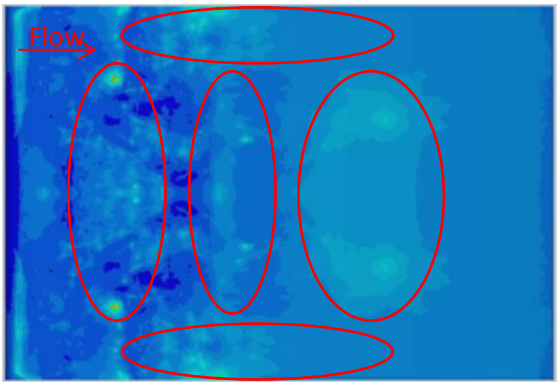

Figure 10. Erosion zones predicted by Function 5.

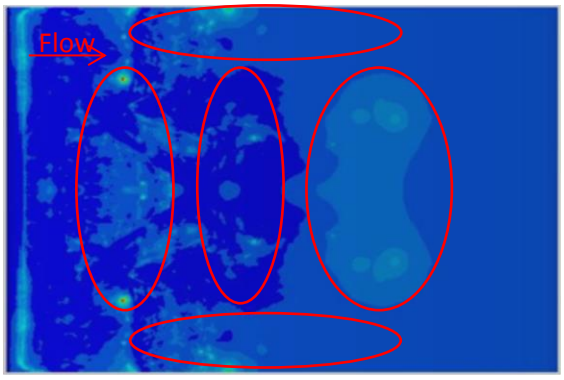

Figure 11. Erosion zones predicted by Function 8.

Undoubtedly, the practical interest lies in the prediction of erosion damage on the ship scale objects, such as propellers and rudders.

3.2. SHIP SCALE: CONTAINERSHIP'S RUDDER

For validation of erosive functions on a ship scale object, a large containership was selected where severe erosion on the rudder had been reported by a ship owner. LR TID performed borescopic cavitation observations on this vessel and identified the areas on the rudder affected by cavitation shed from the propeller. The main paint damage was observed on the port side of the rudder in way of interaction with the propeller hub vortex, as shown in **Figures 18** and **19**.

As the cavitation on the rudder depends on the wake induced by the hull and the propeller, in order to simulate the realistic flow conditions, it was decided to include the hull and the propeller in the calculations.

The hull and propeller geometries were obtained in a high quality IGES file format. The rudder was built separately in STAR-CCM+ using the drawings. In order to be able to mesh the geometries, a generation and repair process of the 3D CAD model was carried out, using the geometry tools included in the STAR-CCM+. **Figure 12** shows the full scale containership simulated in this study.

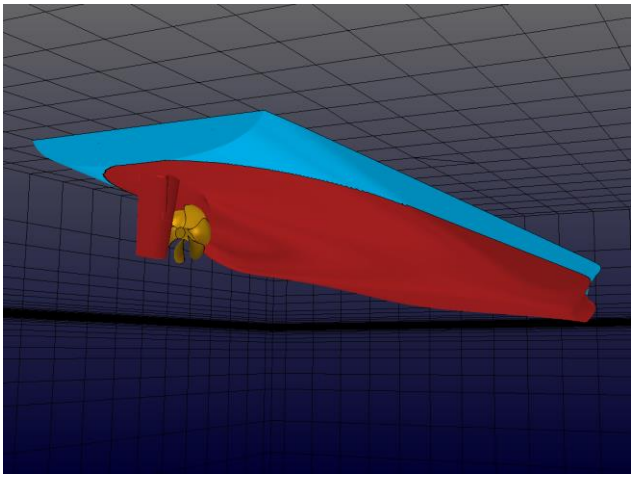

Figure 12. Full scale containership simulated by DES.

As the stern wave had a significant height for the containership, it was necessary to capture the shape of the stern wave, which will influence the hydrodynamic pressure on the propeller blades. In order to reduce the number of cells, the whole analysis was split into two stages. In the first stage of the analysis, the vessel flow was calculated with the free surface in order to determine the shape of the waves. The cavitation model in this stage was not active. **Figure 13** shows the free surface pattern calculated in CFD. Once the calculation was converged, the deformed free surface was exported as a geometrical entity. This free surface geometry was used in the second stage of the calculation and set to an upper symmetry boundary. **Figure 14** shows the free surface with the stern wave. In this stage, the cavitation model was active.

When modelling the physics there are two different regions: one for the hull moving straight and another for the propeller rotating. Therefore, two different mesh regions and connection interfaces were generated.

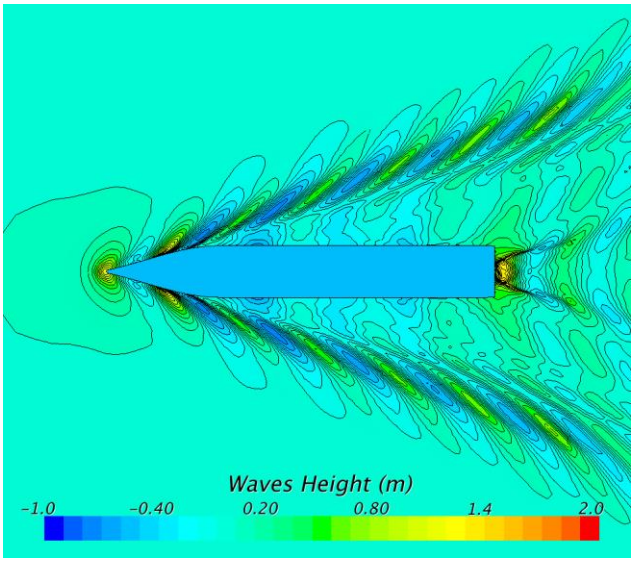

Figure 13. Ship scale free surface pattern.

The overall mesh for cavitation simulation was approximately 16 million cells; 11.5 million of which were in the rotating mesh region. The typical mesh size at hull and rudder surface region was 0.2m, with local refinements down to 0.01m, as shown in **Figure 15**. Local volume refinements behind the blade tips and propeller hub were carried out, in order to capture with high resolution the tip and hub vortex. In addition, the gaps between the rudder horn and the rudder blade were accurately resolved.

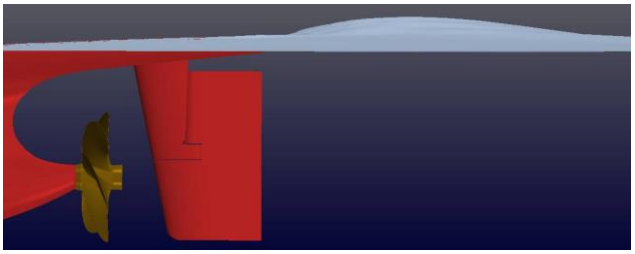

Figure 14. Ship scale stern wave.

Similar to the previous case study, a Detached Eddy Simulation (DES) model was employed to capture the

dynamics of the highly turbulent flow. Propeller rotation was modelled using rigid body rotation of a cylindrical mesh region around the propeller, with sliding interfaces between the static and rotating mesh regions. For the propeller rotation, a second-order temporal differencing scheme was employed for the unsteady term.

As the vessel speed, shaft speed and vessel draughts were recorded during the cavitation observations carried out on the containership, the cavitation analysis was performed at identical conditions.

In order to model the erosive potential, three functions from the model scale study were applied and defined as Function 1, 5 and 8.

An indication of the stability of the solution was confirmed by the evolution of thrust and torque; these quantities were stable over the period of 10 sec and a periodic solution is achieved for both parameters. Another measure of the stability of the solution is the vapour volume for the same period of 10 sec. For thrust and torque, the vapour volume remained stable over the computed period of time.

As mentioned previously, the main paint damage on the rudder surface was caused by the hub vortex originating from the propeller and interacting with the rudder. CFD accurately predicted the formation of the hub vortex and the transportation of the vapour to the rudder, as shown in **Figures 16** and **17**. The simulation confirmed that the hub vortex cavity is relatively stable over the blade passage and collapses on the rudder port side.

A decrease in pressure below saturation appears downstream of the propeller hub, which explains why cavitation appears in the area. This pressure drop is related to an increase of the kinetic energy due to the rotation of the flow**.**

As the views from the borescope positions 1 and 2 (**Figures 18** and **19**) were quite limited due to the water visibility, **Figure 20** shows a schematic area of paint damage on the port side of the rudder.

As can be seen in **Figures 21** to **23,** all erosion functions correctly predicted the paint damage zone observed on the rudder. The area of the port side of the rudder, where the hub vortex interacts with the rudder surface, has noticeable footprints.

As shown in **Figure 21,** the erosion area in the way of the hub vortex is slightly underestimated by Function 1. However, the predictions of Functions 5 and 8 (**Figures 22** and **23**), show a favourable agreement with full scale observations. The brightest footprints of Functions 5 and 8 are located on the port side of the rudder blade in the way of the hub vortex.

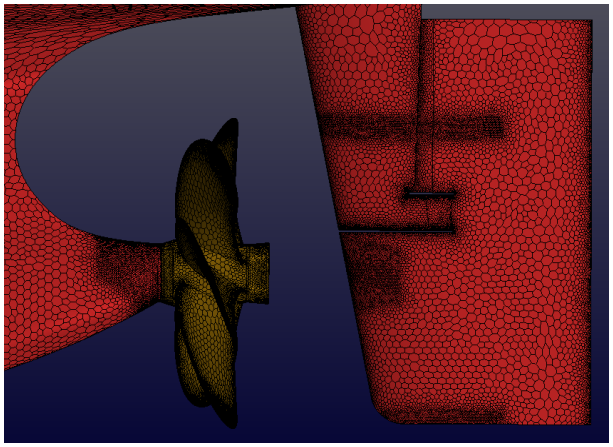

Figure 15. Computational mesh on the propeller and rudder.

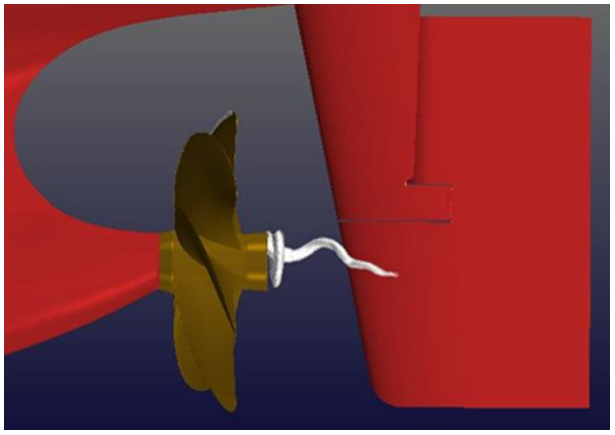

Figure 16. Hub vortex predicted by DES. Port side view.

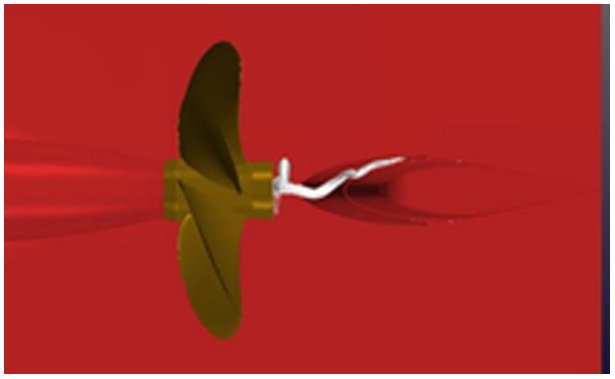

Figure 17. Hub vortex predicted by DES. Bottom view.

Other areas of potential erosion damage, such as the upper part of the horn and lower part of the blade leading edge where the interaction with flow vorticity shed from the propeller blade tips takes place, were also noted. Another bright area of potential damage is the pintle gap between the rudder horn and the rudder blade. However, none are bright enough to suggest the real paint damage.

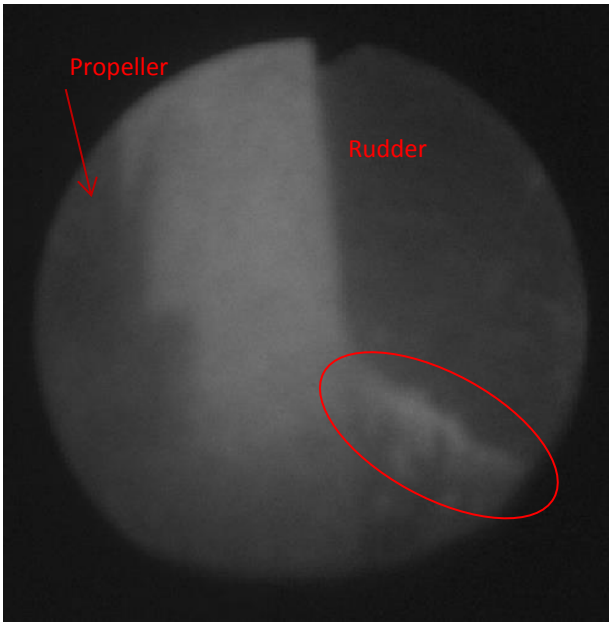

Figure 18. Paint damage on the port side of the rudder observed from the borescope position 1.

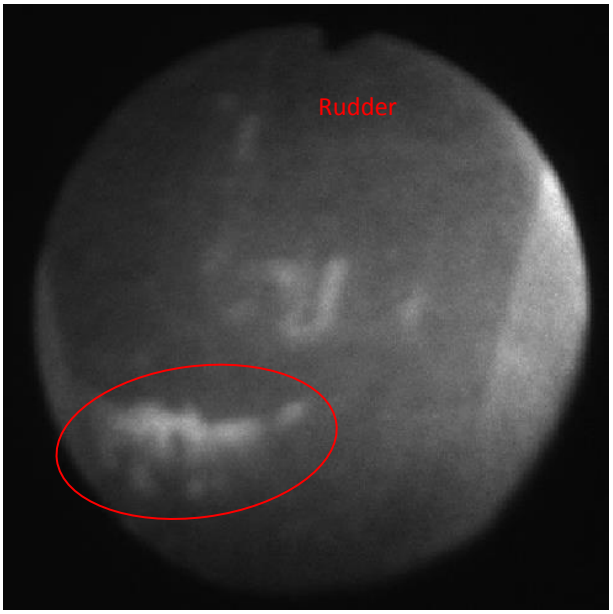

Figure 19. Paint damage on the port side of the rudder observed from the borescope position 2.

4. CONCLUSIONS

LR TID has the technical capability to collect and analyse data from model scale tests as well as full scale trials for the purpose of validating CFD cavitation erosion predictions carried out in-house.

As a result, new erosion functions have been developed and successfully validated against model and ship scale objects.

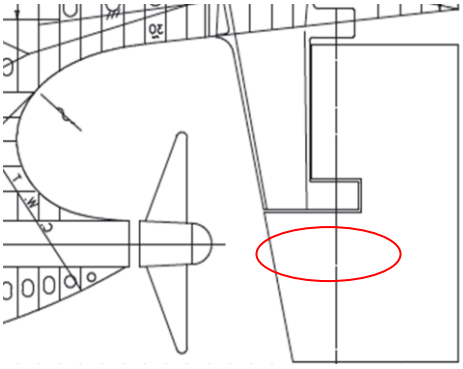

Figure 20. Schematic area of observed erosion damage.

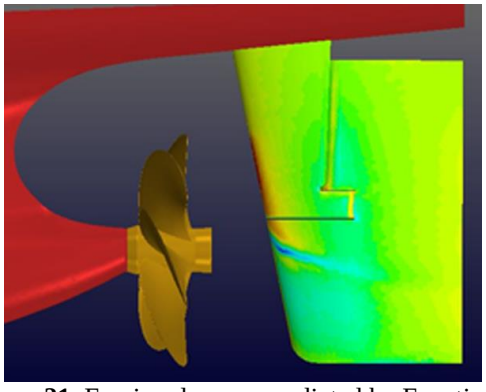

Figure 21. Erosion damage predicted by Function 1.

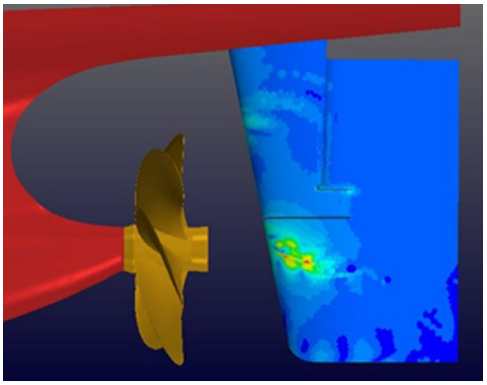

Figure 22. Erosion damage predicted by Function 5.

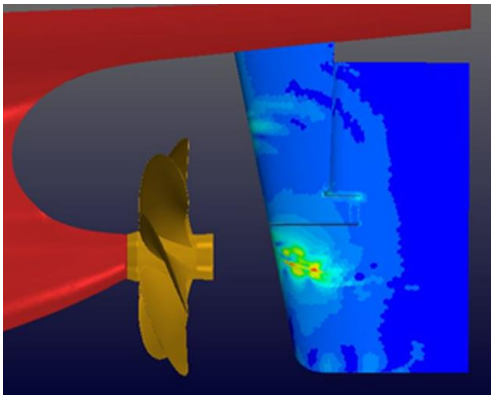

Figure 23. Erosion damage predicted by Function 8.

The simulation of NACA0015 hydrofoil flow using a DES model was carried out in STAR-CCM+ using the same flow conditions used in the cavitation tunnel experiment. The general cavitation behaviour predicted by CFD was relatively accurate; however, the volume of cavitation cloud and the area of its collapse were somewhat underestimated. Nevertheless, the erosion functions showed good results predicting the mechanism of cavity collapse and its effect to the foil surface.

Further validation of erosive functions was performed for a full scale containership's rudder where severe paint damage on the port side was reported by the ship owner.

LR TID performed full scale borescopic observations of cavitation and concluded that the damage on the rudder was caused by interaction with the hub vortex originating from the propeller.

LR TID carried out a CFD simulation of the containership in full scale under the condition recorded during the observations. A DES model was used for the simulation. Erosion functions developed and tested at model scale study correctly predicted the area on the port side of the rudder where the paint damage was reported.

Simplified erosion models, as described in the report, give valuable information about the areas most susceptible to erosion and have proved to be valuable tools at the design stage in order to prevent damage occurring throughout the vessel's life.

It is planned that these functions will be further validated against various cases, in order to provide researchers and ship designers with an affordable and powerful tool for cavitation erosion prediction.

5. ACKNOWLEDGEMENT

The current research project was funded under the internal LR R&D program. The authors would like to thank their colleagues D. Radosavljevic, S. Whitworth, C. Craddock and C. Fetherstonhaugh for their significant support.

6. REFERENCES

Boorsma A., (2010), "Cavitation tests on a NACA 0015 Aerofoil, Quantification of Cavitation Impacts from High Speed Video and AE Signals", CRS Erosion II WG, LR TID report 6997.

Boorsma A, Whitworth S, (2011), "Understanding Details of Cavitation", Second International Symposium on Marine Propulsors, SMP'11, Hamburg, Germany.

Hasuike N., Yamasaki S., Ando J., (2009), "Numerical Study on Cavitation Erosion Risk of Marine Propellers Operation in Wake Flow", Proceedings of the 7th International Symposium on Cavitation CAV2009 – Paper No. 30, Michigan, USA.

Hoekstra M., (2011), "Cavitation Simulations for a NACA0015 foil in a Tunnel", CRS Report 23990-2-RD.

Li Z., (2012a), "Assessment of Cavitation Erosion with a Multiphase Reynolds-Averaged Navier-Stokes Method", PhD thesis, Delft University of Technology.

Li Z., Terwisga T.V., (2012b), "On the capability of a RANS method to assess the cavitation erosion risk on a hydrofoil", Proceedings of the 8th International Symposium on Cavitation CAV2012, Singapore.

Mihatsch M.S., Schmidt S.J., Adams N.A., (2013), "Estimation of incubation times through numerical simulation of 3-D unsteady Cavitating flows", SHF Conference Hydraulic Machines and Cavitation /Air in Water Pipes, Grenoble, France.

Nohmi M., Ikohagi T., Iga Y., (2008), "Numerical Prediction Method of Cavitation Erosion", Proceedings of FEDSM2008, ASME Fluids Engineering Conference, Jacksonville, Florida USA.

Rijsbergen M.X., Boorsma A. (2011), "High Speed Video Observations and Acoustic Impact Measurements on a NACA 0015 Foil", CRS Report 22195-5-RD.

Schmidt S.J., Sezal I.H., Schnerr G.H., Thalhamer M. (2007), "Shock Waves as Driving Mechanism for Cavitation Erosion", Proceedings of the 8th International Symposium on Experimental and Computational Aerothermodynamics of Internal Flows, Lyon.

Schmidt S.J., Sezal I.H., Schnerr G.H., Thalhamer M. (2008), "Numerical Analysis of Shock Dynamics for Detection of Erosion Sensitive Areas in Complex 3-D Flows", Cavitation: Turbo-machinery & Medical Applications, WIMRC FORUM 2008, Warwick University, UK.

Schmidt S.J., Schnerr G.H., Thalhamer M. (2009), "Inertia Controlled Instability and Small Scale Structures of Sheet and Cloud Cavitation", Proceedings of the 7th International Symposium on Cavitation CAV2009 – Paper No. 17, Ann Arbor, Michigan, USA.